

Heavy Ion Fusion at Sub-Barrier Energies: Progress and Questions

R. R. Betts

Physics Division
Argonne National Laboratory
Argonne, IL 60439
USA

RECEIVED
APR 10 1993
CCTI

Invited Paper Presented at RIKEN International Workshop on Heavy-Ion Reactions
with Neutron-Rich Beams, February 18-20, 1993, RIKEN, Saitama, JAPAN

DISCLAIMER

This report was prepared as an account of work sponsored by an agency of the United States Government. Neither the United States Government nor any agency thereof, nor any of their employees, makes any warranty, express or implied, or assumes any legal liability or responsibility for the accuracy, completeness, or usefulness of any information, apparatus, product, or process disclosed, or represents that its use would not infringe privately owned rights. Reference herein to any specific commercial product, process, or service by trade name, trademark, manufacturer, or otherwise does not necessarily constitute or imply its endorsement, recommendation, or favoring by the United States Government or any agency thereof. The views and opinions of authors expressed herein do not necessarily state or reflect those of the United States Government or any agency thereof.

MASTER

cc

DISTRIBUTION OF THIS DOCUMENT IS UNLIMITED

The submitted manuscript has been authored by a contractor of the U. S. Government under contract No. W-31-109-ENG-38. Accordingly, the U. S. Government retains a nonexclusive, royalty-free license to publish or reproduce the published form of this contribution, or allow others to do so, for U. S. Government purposes.

HEAVY ION FUSION AT SUB-BARRIER ENERGIES: PROGRESS AND QUESTIONS

R. R. Betts
Physics Division, Argonne National Laboratory
Argonne, IL 60439 USA

ABSTRACT

The current status of the experimental study of heavy-ion fusion at sub-barrier energies is reviewed. Emphasis is placed on areas of disagreement between experimental data and theoretical predictions. Suggestions for future experiments are discussed.

1. Introduction

Tunneling, the penetration of the wavefunction of a particle into classically forbidden regions, is a fundamental aspect of quantum physics. The passage through potential barriers at energies below the barrier height, which results from this penetration, is a widespread and important process in all aspects of microscopic physics, giving rise to phenomena as diverse as alpha-decay, fission, the behavior of solid-state junctions and effects in molecular physics. It is well known that the presence of coupling of the motion of the particle through the barrier to other degrees of freedom during the tunneling process can have profound effects on the probability of the barrier penetration. In general, the penetration is enhanced at energies below the classical barrier and suppressed above the barrier.

It has been recognized for some years that the process of heavy-ion fusion at energies in the vicinity of the barrier can be quite sensitive to the effects of coupling to other degrees of freedom. This results in the well-known enhancement of fusion cross-sections at sub-barrier energies over the expectations of penetration through simple, one-dimensional potential barriers. The degrees of freedom which are responsible for this enhancement are varied; static deformation of target or projectile, dynamically induced deformations, the transfer of particles etc. etc. Thus, the nuclear case, with the large variety of properties of nuclear ground states, affords a unique opportunity to study this fundamental problem through measurement of the systematic behavior of sub-barrier fusion as a function of the variation of properties of the nuclei involved. Conversely, it might be hoped that our understanding of the phenomenon would shed light on new and interesting features of nuclear structure and dynamics which occur in heavy ion collisions.

From the theoretical standpoint, the "Standard Model" of heavy-ion fusion is Coupled-Channels. This approach considers the relative motion and internal excitations of the colliding nuclei and their coupling through a series of scattering and coupling potentials. Channels not explicitly included in the coupling scheme are described by imaginary components in the scattering potentials. Fusion is

deemed to have occurred by the non-appearance of flux in the channels included in the coupling scheme. This approach has been quite successful in many cases. There are, however, some general questions which might be raised. First, the only degrees of freedom included in this approach, as formulated at present, are those of the separated nuclei and thus any degrees of freedom unique to the di-nuclear or composite system are naturally excluded. For example, coupling to deep-inelastic degrees of freedom. Second, as mentioned the non-included degrees of freedom are contained in the imaginary part of the scattering potentials and therefore any important non-fusion channel which is not included in the coupling scheme, would be counted as "fusion". Thus, identification of these other degrees of freedom and their inclusion in the theory is an important question for the future.

2. Cross-Sections

2.1 Fusion

The classic example of sub-barrier fusion enhancement is that of $^{16}\text{O} + \text{A}^{\text{Sm}}$ ^{1,2}. As is well-known, the magnitude of the sub-barrier fusion varies dramatically with the deformation of the Sm target nucleus. The cross-section for spherical ^{144}Sm is almost two orders of magnitude smaller than that for the well-deformed ($\beta_2 = 0.27$) ^{154}Sm in the sub-barrier region. These cross-section data have been well accounted for by a simple deformed potential model³ and by more detailed coupled channels calculations⁴.

Another important example of the phenomenon is $\text{A}^{\text{Ni}} + \text{A}^{\text{Ni}}$ ⁵, shown in Fig. 1 in comparison with the results of coupled-channels calculations^{6,7}. The enhancement observed for the symmetric systems $^{58}\text{Ni} + ^{58}\text{Ni}$ and $^{64}\text{Ni} + ^{64}\text{Ni}$ is reasonably well accounted for by the model calculations which include couplings to one- and two-phonon quadrupole and octupole vibrations in target and projectile although there is still some underprediction of the data immediately below the classical barrier. For the non-symmetric $^{58}\text{Ni} + ^{64}\text{Ni}$ system, however, despite the inclusion of a number of transfer channels, the model calculation still fails to correctly predict the observed sub-barrier enhancement.

Similar failures of the coupled-channels approach have been noted elsewhere. In a systematic study of symmetric and near symmetric systems near $\text{Zr} + \text{Zr}$, Keller et al.,⁸ observed strong variations of the sub-barrier enhancement with a change of only a few nucleons to the target or projectile. These variations cannot be accounted for by currently available calculations and most probably reflect not only the neglect of deep-inelastic degrees of freedom in the current theoretical treatments, but also a surprisingly strong variation of the importance of these processes with the nuclear structure of target and projectile.

Another system which highlights the differences between experiment and theory is $^{64}\text{Ni} + ^{100}\text{Mo}$ ⁹, shown in Fig. 2. In this case, agreement between the experimental cross-sections and the predictions of a simplified coupled-channels program¹⁰, could only be obtained by artificially increasing the strengths of the coupling to inelastic channels. As will be seen, however, this calculation still fails to reproduce other aspects of the data.

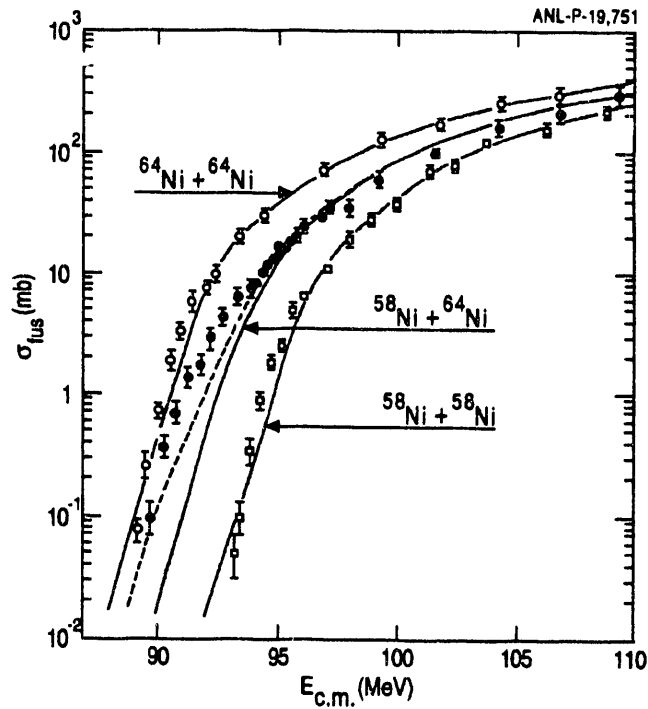


Fig. 1. Fusion cross-sections for $^{58}\text{Ni} + ^{58}\text{Ni}$, $^{58}\text{Ni} + ^{64}\text{Ni}$ and $^{64}\text{Ni} + ^{64}\text{Ni}$. The curves show the results of coupled channels calculations including vibrational excitations (solid) and with the addition of transfer (dashed).

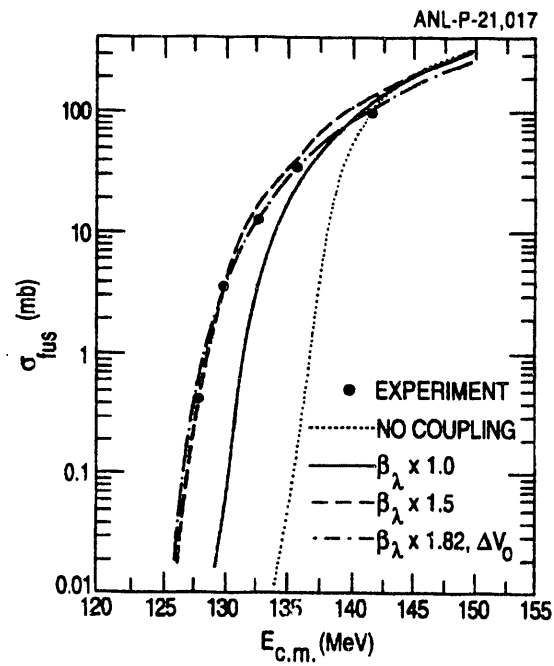


Fig. 2. Fusion cross-sections for $^{64}\text{Ni} + ^{100}\text{Mo}$ in comparison with the results of various calculations.

There are many other examples of both agreement and disagreement between experimental and theoretical sub-barrier fusion cross-sections. To date, no simple phenomenology has emerged which would allow us to know what to expect in a given case. It is clear that the transition between agreement and disagreement occurs quite rapidly, in some cases, with only a small change in the mass of target and projectile. The systematic behavior of this transition and its correlation with properties of the target, projectile and composite system remain to be demonstrated.

2.2 Non-Fusion

As discussed in Sec. 1, the coupled channels formalism, in principle, provides a complete description of all reaction channels and as such should not only describe the behavior of fusion in the sub-barrier region but also elastic and quasi-elastic reaction channels to the extent that these are included in the coupling scheme. Of particular interest in this regard are particle-transfer reactions in that they are expected to play a crucial role in cases such as $^{58}\text{Ni} + ^{64}\text{Ni}$ which, as discussed in Sec. 2.1, represents an outstanding discrepancy between theory and experiment. The effects on fusion of the inclusion of transfer to the coupled-channels scheme were shown in Fig. 1. From the same calculation, Fig. 3 shows the comparison with data¹¹ for one-neutron transfer. This comparison demonstrates the importance of the two-neutron transfer channel on the one-neutron transfer cross-section, a process which also provides a significant additional enhancement in the sub-barrier fusion for this system. Note, however, that these transfer data are measured at energies above even the one-dimensional fusion barrier. Data in the region of energies where the measured fusion cross-section deviates most from theory ($90 < E_{\text{cm}} < 95$ MeV) would be of great interest.

In general, measurement by conventional means of quasi-elastic processes at sub-barrier energies is difficult due to problems detecting the low-energy reaction products scattered to large angles. Using a recoil mass separator to detect the target-like fragment, which is produced recoiling to forward angles with relatively high energy^{12,13}, it has been possible to measure one and two particle transfer reactions far into the sub-barrier region. Cross-sections for one-neutron pickup in $^{58}\text{Ni} + \text{Sn}$ are shown in Fig. 4 plotted versus center-of-mass bombarding energy, together with the predictions of a simple semi-classical model of the transfer process (which is itself a barrier penetration phenomenon). The strong dependence of the transfer probability as a function of target mass is found to result from the changing ground-state Q-value for this channel and this is also reflected in the isotopic dependence of the sub-barrier fusion for these systems.

Although, in the case of $^{58}\text{Ni} + \text{Sn}$, it appears that the one neutron transfer couples directly to the fusion, it should not be assumed that just because a particular reaction channel is strong it necessarily has a large effect on fusion. What could be the case is that the channel in question plays the part of a "doorway" to more complex channels which in turn couple to fusion. For example, the transfer of neutrons most likely forms the first step in the transfer of many nucleons and thus, if this first step is closed due to structural or dynamic reasons, none of the subsequent transfers can take place. This is of some interest as, in the case of $^{58}\text{Ni} + \text{Sn}$, substantial deep-inelastic transfer cross-sections have been

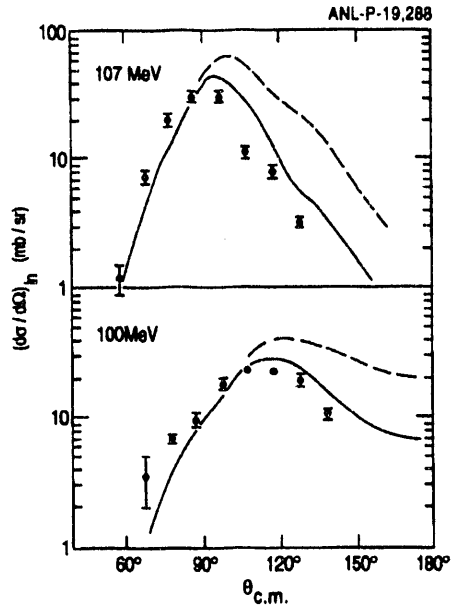


Fig. 3. One-neutron transfer angular distributions for $^{58}\text{Ni} + ^{64}\text{Ni}$ in comparison with the results of coupled channels calculations. The solid curve shows the effects of including sequential two-neutron transfer in the coupling scheme.

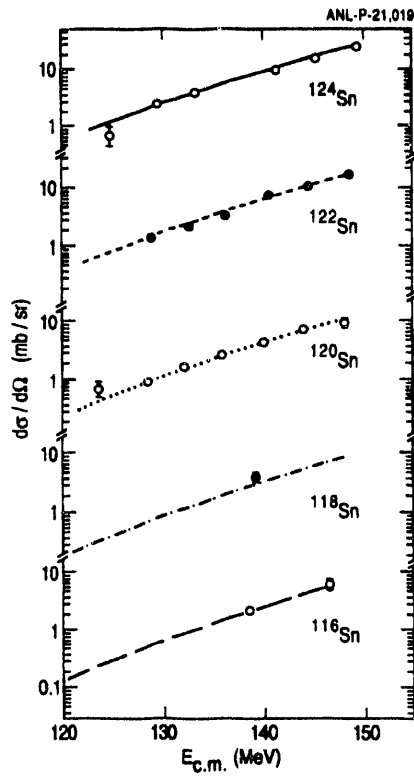


Fig. 4. Excitation functions at $\theta_{\text{c.m.}}=180^\circ$ for $^{58}\text{Ni} + ^A\text{Sn}$ one-neutron transfer. The curves show the results of a semi-classical calculation of the neutron transfer.

observed^{14,15} at energies close to the barrier. It will be of interest to see if the behavior of the few nucleon quasi-elastic cross-sections is reflected in the deep inelastic cross-sections for these systems.

With this in mind, the new generation of recoil mass separators (Legnaro, Argonne ...), with their larger dynamic range and acceptance in A/q , can be used to probe the transition from quasi-elastic to deep-inelastic processes and the subsequent connection to fusion. Data¹⁶ for $^{58}\text{Ni} + ^{154}\text{Sm}$ at 260 MeV bombarding energy is shown in Fig. 5, demonstrating the use of time-of-flight through the separator to resolve different charge states of the target-like recoils and reveal the transfer of up to four nucleons from the target to projectile. The time-of-flight can also be used to reconstruct the Q-value distribution of these transfers which show a transition from a quasi-elastic like behavior for the one and two nucleon transfers to a much more strongly damped behavior for nucleon transfer of more than two.

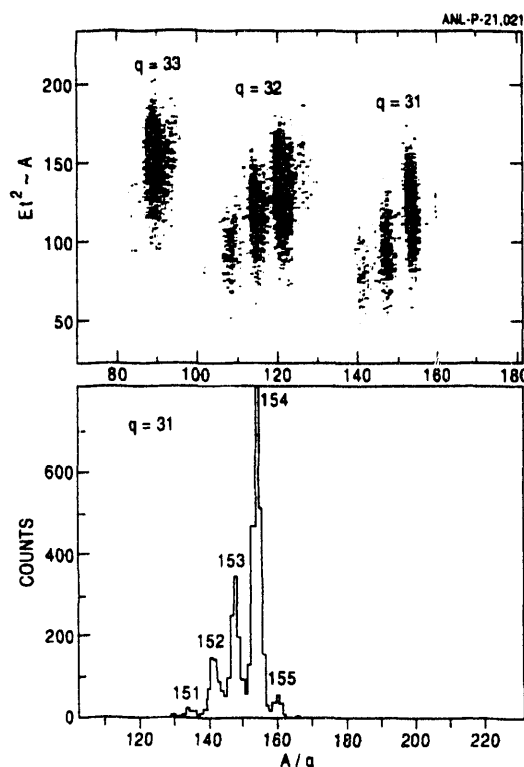


Fig. 5. Upper - A/q versus Et^2 for $^{58}\text{Ni} + ^{154}\text{Sm}$, target-like, recoils at a bombarding energy of 260 MeV.
Lower - Projection on the A/q axis for charge state $q=31$.

Further experimental studies of this type will be very important in the overall picture of sub-barrier fusion and its relation to other reaction channels.

3. Spin Distributions

In addition to the total fusion cross-sections themselves, the partial wave distribution of the fusion cross-section provides an additional and often crucial test of theoretical models. For example, it has been shown¹⁷ that two different models which predict identical total fusion cross-sections - adjusted barrier and coupled channels - for the $^{40}\text{Ar} + ^{122}\text{Sn}$ system have distinctly different predicted spin distributions close to and below the barrier.

Several different techniques have been used to determine the compound nucleus spin distribution following fusion; isomer ratios, rotational band population, gamma-ray multiplicities and fission fragment angular distributions. These techniques have been summarized in a recent review¹⁷. A typical behavior deduced from these measurements is shown in Fig. 6 where the mean angular momentum derived¹⁸ from gamma-ray multiplicity distributions is shown plotted versus bombarding energy for $^{28}\text{Si} + ^{154}\text{Sm}$ and is compared with theoretical predictions. At energies close to and below the barrier the mean angular momentum shows a characteristic "bump" which is correlated with the deviation of the measured fusion cross-sections from the one-dimensional barrier predictions. In this case, the magnitude of the "bump" and the return of the value of the mean

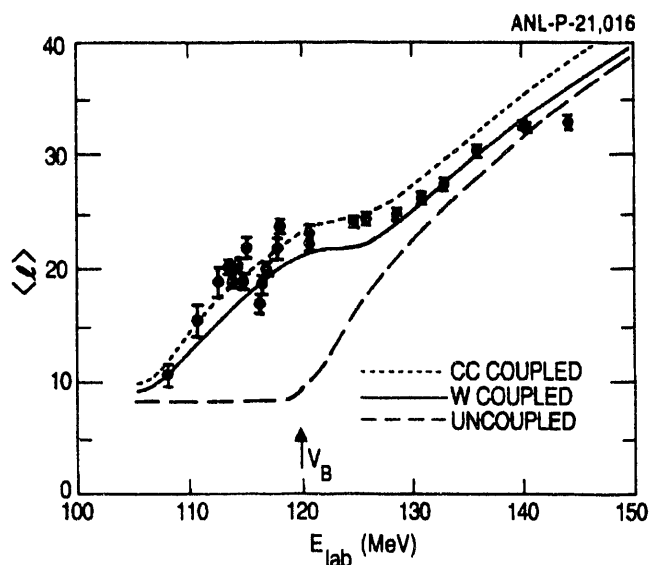


Fig. 6. Energy dependence of the mean angular momentum of the compound nucleus for $^{28}\text{Si} + ^{154}\text{Sm}$ fusion. The curves show the results of simple barrier penetration (dashed), deformed barrier (solid) and coupled-channels (short-dashed) calculations.

angular momentum to the uncoupled value at low energies is correctly described by theory. Although there are many aspects of relationship between gamma-ray multiplicities and spin distributions which might be criticized, it is unlikely that there are any major errors in the spin distributions obtained in this way. Indeed, in the case of $^{16}\text{O} + ^{152}\text{Sm}$ ¹⁹, the spin distribution derived from gamma-ray multiplicities

complete agreement with that predicted by theory. The existence of significant discrepancies between theory and experiment are therefore to be taken seriously.

For a number of systems, $^{64}\text{Ni} + ^{92,96}\text{Zr}_{20,21}$ and $^{64}\text{Ni} + ^{100}\text{Mo}_9$, the features of the experimentally determined spin distributions in the barrier region show major deviations from current theoretical expectations. Data for $^{64}\text{Ni} + ^{100}\text{Mo}$ is shown in Fig. 7 compared with the results of the same calculations shown with the cross-section data in Fig. 2. Even the calculation with the inelastic coupling strength scaled by 50% fails to account for the high values of $\langle l \rangle$ and $\langle l^2 \rangle$ below the barrier. This failure is most likely related to the importance of deep inelastic degrees of freedom in these massive, near symmetric systems and their neglect in the calculations. The understanding of this discrepancy is a major question for the future.

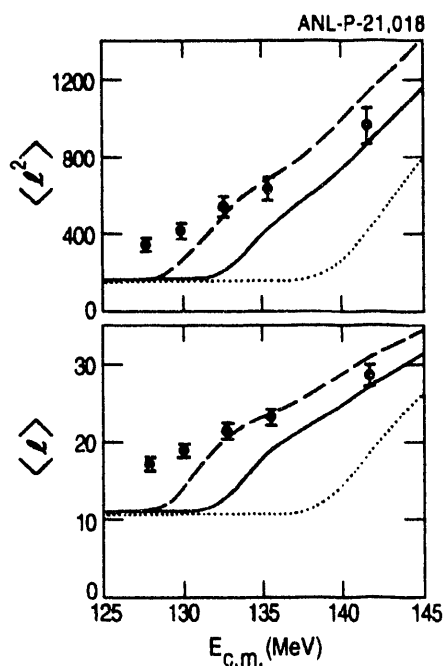


Fig. 7. Energy dependence of $\langle l \rangle$ and $\langle l^2 \rangle$ for $^{64}\text{Ni} + ^{100}\text{Mo}$ fusion. The curves refer to the same calculations as in Fig. 2.

Even though it appears that there is no major flaw in the extraction of spins from gamma-ray multiplicity data, it is important to have confidence in the technique. Here, the potential availability of radioactive beams gives us a possibility for a direct test of the precision with which spin distributions can be determined. With a beam or target with spin, in the absence of significant spin-orbit coupling, higher spin states are populated in the compound nucleus than would be the case for spinless target and projectile. The probability of barrier penetration is, however, the same as it would be in the spinless case and thus a high-spin beam or target provides a way of introducing an additional, model-independent contribution to the spin distribution. The ability of measurement to detect this increase is an important

test of the sensitivity and precision of the technique used. For a beam of spin j incident on a spinless target, the compound nucleus cross-section for spin J is given by:

$$\sigma(J) = \pi \lambda^2 \sum_{\ell=|J-j|}^{J+j} \frac{(2J+1)}{(2j+1)} T(\ell)$$

where $T(\ell)$ is the barrier transmission coefficient for orbital angular momentum ℓ . The effect of this coupling is shown in Fig. 8 where a sharp cutoff spin distribution with $\ell_{\max}=10$ is compared with the spin distribution expected for a $j=5$ projectile and the same transmission coefficients. The mean spin increases from 6.8 to 8.4 \hbar . Beams which might be used in this way are many. ^{26}Al ($j=5$, $\tau=7 \times 10^5$ y) is a conveniently long lived case although other high-spin ground-state and metastable state beams with half lives in the range seconds to minutes are common.

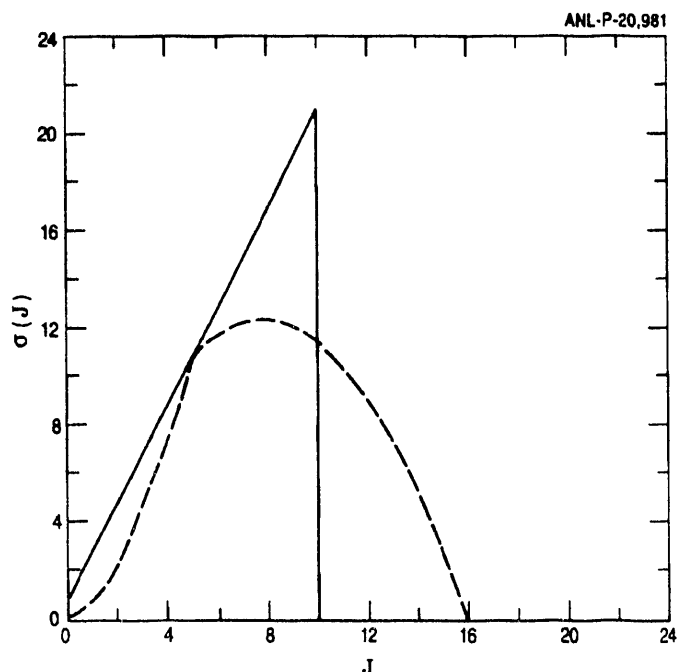


Fig. 8. Spin distributions calculated for a sharp cutoff in transmission coefficients with $\ell_{\max}=10$ for a projectile spin of zero (solid) and 5 (dashed).

Another technique which has been used to obtain information on spin distributions is the measurement of fission-fragment angular distributions. The standard theory of fission fragment distributions assumes that an equilibrium of orientations of the fissioning system relative to the angular momentum is established at the saddle point. Studies^{22,23} of ^{12}C and ^{16}O induced fission analyzed in the standard framework have led to anomalously large values of the mean angular momentum in the barrier region. This is a perplexing result as, for such light projectiles, the standard theories are usually well able to account for the spin distributions, at least for lighter targets. It is therefore important to know

whether or not these results constitute a failure of sub-barrier fusion theory or rather reflect some deficiency in our understanding of the fission process. A possible test of these data arises again from the adding of angular momentum to the system through the use of target and projectiles with spin and seeing if this is correctly reflected in the measured mean spins of the compound nucleus. For the case of $^{16}\text{O} + ^{208}\text{Pb}$ fission, studied in Ref. 23, it is possible to make the same fissioning system via the $^{15}\text{N}(j=3/2)+^{209}\text{Bi}(j=9/2)$ and the $^{14}\text{N}(j=1)+^{210}\text{Bi}^m(j=9)$ entrance channels. The effects of these entrance channels on a spin zero sharp cutoff distribution ($\ell_{\text{crit}}=10$) are shown in Fig. 9. In this case the compound nucleus

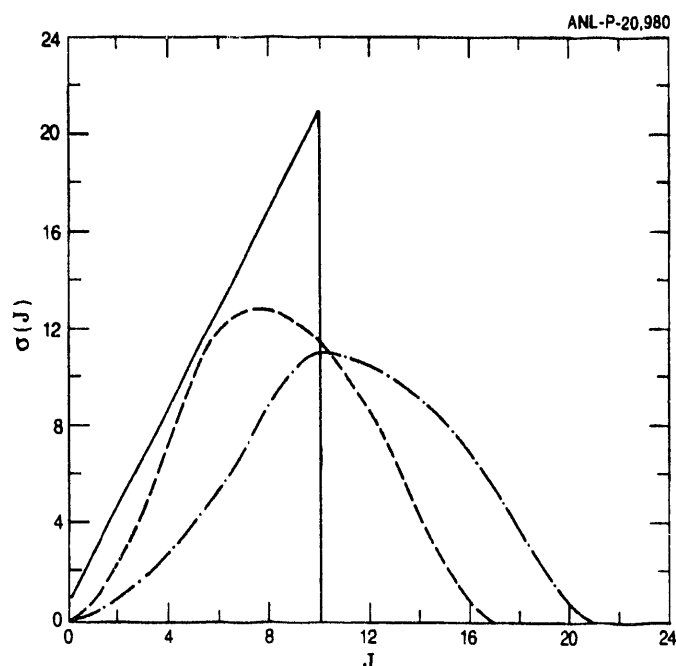


Fig. 9. Spin distributions calculated with a sharp cutoff in transmission coefficients with $\ell_{\text{max}}=10$ for $^{16}\text{O} + ^{208}\text{Pb}$ (solid), $^{15}\text{N} + ^{209}\text{Bi}$ (dashed) and $^{14}\text{N} + ^{210}\text{Bi}^m$ (dot-dash).

cross-section for spin J is given by:

$$\sigma(J) = \pi \bar{\kappa}^2 \sum_{\ell=|J-(j_1+j_2)|}^{J+(j_1+j_2)} \frac{(2J+1)}{(2j_1+1)(2j_2+1)} T(\ell)$$

where j_1 and j_2 refer to the projectile and target spin. In the three cases, the mean compound nucleus increases from 6.8 ($^{16}\text{O} + ^{208}\text{Pb}$) to 8.3 ($^{15}\text{N} + ^{209}\text{Bi}$) to 11.2 ($^{14}\text{N} + ^{210}\text{Bi}^m$).

The effect on the fission fragment angular distribution not only depends on the increased angular momentum but also on the distribution of the projection of J on the beam axis which makes the predicted fission angular distributions a more

complex function of J than is the case for spinless target and projectile. Nevertheless, there should be observable differences between the three cases which provide a model independent test of the angular distribution theory and therefore determine whether the reported large values of the average angular momentum are in fact correct. If the previously reported large values of the mean angular momentum hold up, these cases constitute a major discrepancy with theory.

4. Summary

Although the general aspects of the physics underlying heavy-ion fusion in the sub-barrier region are not in question, there exist outstanding discrepancies in the comparison between experiment and theory. The resolution of these differences requires much work, both experimental and theoretical. Important issues are:

- More detailed data on fusion cross-sections, particularly for heavier projectiles, defining the boundaries of agreement and disagreement with theory.
- Data on quasi-elastic and deep-inelastic process in the barrier region and their correlation with fusion.
- Inclusion of more complex degrees of freedom (necking, deep-inelastic ..) in the theory of sub-barrier fusion.
- Testing of the validity of simplified calculations which have been used to mimic full coupled-channels treatments.
- Experimental tests of the methods of determining spin distributions from gamma-ray multiplicities and fission angular distribution.
- More data on spin distributions in the barrier region and the correlation of the anomalous results with cross-sections in the fusion and non-fusion channels.

This is an ambitious program. The problem is, however, an important one with implications for a wide range of physics questions.

Acknowledgment

This work was supported by the U.S. Department of Energy, Nuclear Physics Division, under contract W-31-109-ENG-38.

References

1. R. G. Stokstad et al., *Phys. Rev. Lett.* **41** (1978) 465.
2. D. E. DiGregorio et al., *Phys. Lett.* **B176** (1986) 322.
3. C. Wong, *Phys. Rev. Lett.* **31** (1973) 766.
4. H. Esbensen, *Nucl. Phys.* **A352** (1981) 147.
5. M. Beckerman et al., *Phys. Rev. Lett.* **45** (1980) 1472.
6. H. Esbensen and S. Landowne, *Phys. Rev.* **C35** (1987) 2090.
7. H. Esbensen and S. Landowne, *Nucl. Phys.* **A492** (1989) 473.
8. J. G. Keller et al., *Nucl. Phys.* **A452** (1986) 173.
9. M. L. Halbert et al., *Phys. Rev.* **C40** (1989) 2558.
10. CCFUS, C. H. Dasso and S. Landowne, *Phys. Lett.* **B183** (1987) 141.
11. K. E. Rehm et al., *Phys. Rev. Lett.* **55** (1985) 280.
12. R. R. Betts et al., *Phys. Rev. Lett.* **59** (1987) 978.
13. C. N. Pass et al., *Nucl. Phys.* **A499** (1989) 978.
14. F. L. H. Wolfs et al., *Phys. Lett.* **B196** (1987) 113.
15. F. L. H. Wolfs et al., *Phys. Rev.* **C36** (1987) 1379.
16. M. Freer et al., (unpublished).
17. R. Vandenbosch, *Ann. Rev. Nucl. Sci.* **42** (1992) 447.
18. S. Gii et al., *Phys. Rev. Lett.* **65** (1990) 3100.
19. A. H. Wuosmaa et al., *Phys. Lett.* **B263** (1991) 23.
20. A. M. Stefanini et al., *Nucl. Phys.* **A538** (1992) C195.
21. W. Kühn et al., *Phys. Rev. Lett.* **62** (1989) 1103.
22. R. Vandenbosch et al., *Phys. Rev. Lett.* **56** (1986) 1234.
23. T. Murakami et al., *Phys. Rev.* **C34** (1986) 1353.

**DATE
FILMED**

6 / 17 / 93

